Proceedings of the 2015 International Conference on Machine Learning and Cybernetics, Guangzhou, 12-15 July, 2015

A REAL-TIME PARALLEL COMBINATION SEGMENTATION METHOD FOR ALUMINUM SURFACE DEFECT IMAGES

XIU-QIN HUANG [1], XIN-BIN LUO [1,2], REN-ZHONG WANG[1]

[1] Suzhou Non-ferrous Metals Research Institute, Suzhou, Jiangsu, China
[2] School of Aeronautics and Astronautics, Shanghai Jiaotong University, China
E-MAIL: huangxiuqing@163.com, losinbin@163.com

Abstract:

A single defect image segmentation algorithm cannot obtain the desired segmentation results for all images because of the defect diversity. A parallel combination segmentation method is proposed to integrate multiple results of the different segmentation algorithms to obtain the desired defect segmentation map for high-speed aluminum surface defect detection. Two types of segmentation algorithms are designed in this combination framework, namely, the automatic threshold segmentation based on the image statistical model and adaptive entropy-based segmentation. The automatic threshold segmentation algorithm detects defects rapidly using the threshold parameters obtained by modeling the image effectively, and the adaptive entropy-based segmentation algorithm effectively detects defects using 1D information entropy. These two types of segmentation algorithms run in parallel, and their segmentation results are fused by an "and" operation. Thus, an improved image segmentation map with higher accuracy is obtained. Many experimental results and field applications show that the parallel combination segmentation algorithm is a stable and efficient segmentation algorithm, which improves the accuracy of the original segmentation algorithm that it contains.

Keywords:

Combination segmentation; Edge detection; Defect extraction; Surface defect detection; Entropy

Defect segmentation plays a key role as a bridge between defect image pre-processing and advanced analysis of machine vision in a defect detection system. It is the foundation of the subsequent high-level processing such as defect feature extraction, defect identification, and classification.

Several segmentation algorithms have been proposed [1–4], which are widely used in the aerospace, biomedical engineering, industrial inspection, robot vision, police judiciary, military guidance, culture and arts, mapping, and other geographical areas. Traditional image segmentation algorithms are generally divided into three primary categories: threshold-based segmentation [1], edge detection segmentation [2], and region segmentation [3, 4]. The global threshold segmentation algorithm is the easiest with the fastest computing speed among these segmentation algorithms, especially when the contrast between the target and background is high. This condition generally obtains a unicom and closed segmentation area or segmentation area that contains multiple objects. However, the disadvantage of the thresholding technique is also clear, wherein the threshold selection becomes impossible in a complex image background and dynamic process. Besides, this method only considers the gray pixel itself and ignores the image of the spatial correlation characteristics. Its segmentation results are easily affected by noise interference. Edge detection is also selected for this extraction task, which is performed by detecting the boundary of the enclosed area of the image segmentation. Such a method based on the edge detection operator easily produces much noise and pseudo defects, and the edges extracted are discontinuous, especially for the non-uniform image. Regional growth and division consolidation method are two typical serial regional technical approaches that determine the next steps according to the results of previous steps during its segmentation process. Regional growth starts from a point or some pixels and finally obtains the entire region, which achieves the target extraction. For the division consolidation method, the split and merge process is almost the opposite of regional growth: it starts from the entire image, constant splitting obtains sub-regions, and then the foreground regions are merged to realize object extraction. The regional growth method is computationally simple and can obtain an ideal segmentation result for a uniform connectivity image. However, it has to determine the seed point and is sensitive to noise, which can also generate a hole in the region. In addition, it is a serial algorithm, wherein the segmentation speed is slow when the target is large. The split and merge method can obtain satisfactory segmentation results for a complex image, but the algorithm is more complex, computationally intensive, and a split can undermine the border area.

978-1-4673-7220-6/15/$31.00 ©2015 IEEE

Given the diversity of defects and limitations of each segmentation algorithm, a single algorithm cannot easily obtain suitable segmentation results for all images. Several images can be suitable for this segmentation method, whereas other images can be suitable for another method. Therefore, how to integrate different segmentation methods and design an effective combination of segmentation method to improve segmentation accuracy has become the focus of mainstream research [5]. This study develops a combined image segmentation method for metal strip surface defect detection, which attempts to effectively address the complexity of the defects and image background. This method then improves the final segmentation accuracy and ultimately meets the real-time requirements of the detection system.

We adopt two types of segmentation algorithms according to the specific characteristics of aluminum surface defects and detection system requirements: the automatic threshold segmentation based on the statistical model, and the adaptive entropy-based segmentation. These two image segmentation algorithms are run in parallel, and then the two segmentation results are finally fused by an "and" operation to obtain the final segmentation results.

This paper is organized as follows: Section 2 describes the proposed parallel combined segmentation method; Section 3 analyzes the experimental results; and Section 4 provides the conclusions.

1. Parallel Combined Segmentation

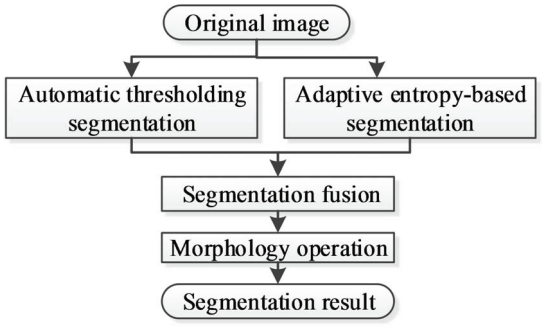

Figure1. Segmentation flowchart

The parallel combined segmentation method is proposed to obtain better segmentation results than the single segmentation method by maximizing the advantages of different algorithms. We designed two segmentation algorithms in our alumina surface defect detection system, namely, the automatic thresholding segmentation and adaptive entropy-based segmentation. Both algorithms run in parallel to complete the image segmentation task separately, and then their segmentation results are fused to provide a new target defect area. Finally, morphological operation is used to improve the final segmented defect regions. The flowchart of the defect segmentation is shown in Figure 1.

1.1 Automatic threshold segmentation based on the image model

Given the continuous changes in the imaging environment, the background of the image varies with different images. We should model the image adaptively, that is, compute the model parameters for each image. The image background of a defect image is more uniform and Gaussian for most images compared to the defect itself. Thus, we use the Gaussian model for the image background. The Gaussian model is described by the following probability density function:

$$f(x) = \frac{1}{\sigma\sqrt{2\pi}} e^{-\frac{1}{2}(\frac{x-\mu}{\sigma})} \quad (1)$$

where x is the variable of the image gray value, parameter μ is the mean, and parameter σ is the standard deviation. The two parameters μ and σ completely specify the distribution.

The location of the image defect is usually in the middle of the image, and its area is generally not much smaller than the background or even larger than the background. Thus, using the entire defect image to model the image background is unsuitable. We designed a group rectangle on the image to select certain pixels from the image as a sample for the image model. These rectangles are in the periphery of the defect, that is, the defect is in the area of the rectangles. When the size and position of the rectangle in the image is set appropriately, the defect proportion on the rectangular sides is small. The variance illustrates the data fluctuation and stability. A smaller variance indicates that the pixels come from one class, that is, the background class with higher probability. We collected the pixels on the rectangular sides with minimum variance as the sample for the image model. The process of model parameter computation is a process that determines the values to represent the image background. The final computed mean value is called the background value, and its algorithm is as follows:

1) The rectangle position parameters are initialized: the start point is (x_0, y_0) , the space distance is l , and the total number of rectangles is j . The point (x_0, y_0) value is generally small and almost the starting point for the top right corner of the image, such as $(x_0, y_0) = (0,0)$ or $(x_0, y_0) = (0,1)$.

2) Data sets are created by a rectangle group for model parameters:
   (1) The first rectangle is drawn on the image: the start point (x_0, y_0) is the top left vertex of the rectangle, whereas point $(M-1-x_0, N-1-y_0)$ is the bottom right vertex of the rectangle. The first rectangle is denoted by $R_1 = (x_0, y_0; M-1-x_0, N-1-y_0)$, and the pixels on the four sides of rectangle R_1 are collected as the first training data set.
   (2) Other rectangles and data sets are created by parallel movement of the four sizes of the rectangle: the second rectangle is denoted by $R_2 = (x_0+l, y_0+l; M-1-x_0-l, N-1-y_0-l)$, …., and the j-th rectangle is denoted by $R_j = (x_0+(j-1)\cdot l, y_0+(j-1)\cdot l; M-1-x_0-(j-1)\cdot l, N-1-y_0-(j-1)\cdot l)$.
   (3) The mean and variance of the abovementioned j data sets are computed: the mean of each set is $\mu_1, \mu_2 ..., \mu_j$, whereas the variance of each set is $\sigma_1^2, \sigma_2^2, ..., \sigma_j^2$.
   (4) The maximum of sets $\{ \sigma_1^2, \sigma_2^2, ..., \sigma_j^2 \}$, $m = \arg\max(\sigma_i^2)$ is computed, and then rectangle R_m is deleted from sets $\{ R_1, R_2, ..., R_j \}$. New rectangle sets $\{ R_1, ..., R_{m-1}, R_{m+1}, ..., R_j \}$ are obtained.
   (5) The pixels on the rectangle sets $\{ R_1, ..., R_{m-1}, R_{m+1}, ..., R_j \}$ are collected as sample set S for the background image model parameter calculation ,
3) The mean μ and variance σ of the sample set S are computed.

The image background model can then be specified by the parameters μ and σ.

We set adaptive threshold values for segmentation based on the Gaussian model for each image using the parameters μ and σ. An empirical rule of Gaussian distribution states that almost 99.7% of the data falls within three standard deviations of the mean. We introduce two coefficients, η_1, η_2 ($\eta_1 \in R^+, \eta_2 \in R^+$) based on this rule to control the inspection sensitivity. The smaller $\eta_i (i = 1, 2)$ is, the higher the sensitivity becomes and more defects detected. After non-uniformity correction in each image, the background value of the corrected image is computed and the corrected image is segmented by the following function:

$$f(x) = \begin{cases} 1 & if\ x \in [0, \mu - \eta_1\sigma) \cup (\mu + \eta_2\sigma, 255] \\ 0 & if\ x \in [\mu - \eta_1\sigma, \mu + \eta_2\sigma] \end{cases} \quad (2)$$

where the value index represents the defect, and the 0 index represents the background. If $\eta_i = 3 (i = 1, 2)$, then almost 99.7% of the image pixel falls within the range of $[0, \mu - 3\sigma) \cup (\mu + 3\sigma, 255]$, which is labeled as the background.

1.2 Adaptive entropy-based segmentation

Many entropy-based thresholding methods have been proposed by researchers in recent years [6, 7], wherein several are based on Shannon's entropy concept. Shannon's entropy concept [8] states that the image of the normal aluminum surface is informationless and the image entropy is almost zero. If defects appear on the aluminum surface, the corresponding image entropy becomes larger for more informational regions. These methods attempt to compute the optimal threshold value. The entropy-based thresholding basically selects an optimal threshold value according to the statistical measure of the difference in image values. We adopt the segmentation method based on 1D entropy in this work for efficiency. Image entropy has been used in image segmentation to describe how much information of the original unthresholded image is preserved in the thresholded image according to Shannon's theorization of information [8]. The optimal threshold value is computed by maximizing the sum of the target and background entropies [9]. The histogram entropy is a measure of the amount of information associated with the histogram. Unlike conventional approaches, we use the thresholding technique to improve our edge detection provided by the Prewitt operation to remove the non-uniformity effect. We detail the formulation in the following section.

For the image which has been filtered by Prewitt kernel, L is the gray-scale of the $M \times N$ image, the gray value range is $[0, L-1]$, and h_i is the pixel number with the gray value i. The occurrence probability of the gray value i is provided by the following:

$$p_i = \frac{h_i}{\sum_{i=0}^{L-1} h_i} = \frac{h_i}{M \times N} = \frac{h_i}{MN} \quad (3)$$

d is denoted as the threshold, A is the boundary edge, and B is the background area. The occurrence probability values of the defect and background targets are then $P_A = \sum_{i=0}^{d} p_i$ and, $P_B = \sum_{i=d+1}^{L-1} p_i$ respectively.

The 1D entropies of the defect target and background are expressed as follows:

$$H(A(d)) = -\sum_{i=0}^{d} (p_i / P_A) \log_2 (p_i / P_A) \quad (4)$$

$$H(B(d)) = -\sum_{i=d+1}^{L-1} (p_i / P_B) \log_2 (p_i / P_B) \quad (5)$$

The information entropy of the image for the threshold value d can de expressed as follows:

$$H(d) = H(A(d)) + H(B(d)) \quad (6)$$

when $p_i = h_i / MN$, $P_A = \sum_{i=1}^{d} p_i$, and $P_B = \sum_{i=d+1}^{L-1} p_i$ are substituted into Equation (4), then $H(d)$ is rewritten as follows:

$$H(d) = -\frac{1}{a}\sum_{i=1}^{d} h_i \log_2 h_i - \frac{1}{MN-a}\sum_{i=d+1}^{L-1} h_i \log_2 h_i + \log_2 (a(MN-a)) \quad (7)$$

Let $a = \sum_{i=1}^{d} h_i$, then $\sum_{i=d+1}^{L-1} h_i = MN - a$. $H(d)$ is then rewritten as follows:

$$H(d) = -\frac{1}{a}\sum_{i=1}^{d} h_i \log_2 h_i - \frac{1}{MN-a}\sum_{i=d+1}^{L-1} h_i \log_2 h_i + \log_2 (a(MN-a)) \quad (8)$$

The optimal threshold value can be expressed as follows:

$$d = \arg\max(H(d)) . \quad (9)$$

Edge detection is enhanced using the following rule with the threshold value d :

$$f(i) = \begin{cases} 0 & i \le d \\ 1 & i > d \end{cases} , \quad (10)$$

where the value 1 indicates the defect target, and the value 0 indicates the background. Edge detection is thus enhanced.

1.3 Parallel combination segmentation

After the defect image is segmented in parallel with the automatic threshold segmentation based on the image model and adaptive entropy-based algorithm, two segmentation results are obtained and denoted as *Z* and *E*. *Z* and *E* are binary images, where 1 is a defect pixel and 0 represents the background pixel. We use an "and" operation to fuse these two binary images, and the fused binary image is denoted as *F*. The fusion process can be represented by the following formula:

$$F(i,j) = Z(i,j) \oplus E(i,j) = \begin{cases} 0 & Z(i,j) = 0 \ and \ E(i,j) = 0 \\ 1 & others \end{cases} \quad (11)$$

A single segmentation method cannot easily consider all the defects, and each algorithm has its own characteristics. Thus, differences between their segmented images exist. Several segmentation algorithms can have better segmentation results for a certain image type, whereas other segmentation algorithms are suitable other image types. When these different methods are combined, they can compensate for each other's shortcomings and improve the segmentation accuracy.

1.4 Morphological operation

The resulting defect detection results after segmenting can contain some random noise and naturally leaves the defect regions as holes. This phenomenon weakens but remains when using a segmentation combination because of complementarity between different algorithms. The morphological operation is used to eliminate the noise, fill the holes, and link the defect fracture. The final defect region is then extracted.

Two structuring elements are selected according to the inherent characteristics of the defects [10,11]. We first remove noise dots or false defects using erosion operation with a square 3 × 3 erosion structure element similar to [10]. We then use the region filling algorithm for hole-filling by the dilation operation with a symmetrical 3 × 3structure element, where the connectivity type is 8-neighborhood. Finally, a diamond-shaped 5 × 5 structure element is used to erode the small particle caused by the hole-filling and improve the final extraction accuracy. These three steps not only connect the parts of the defect but also remove the heterogeneous points in the target

2. Experiment and analysis

We not only make offline tests but also conduct an online test using the image data from an aluminum plant to evaluate the proposed combination segmentation method. The segmentation results of the automatic threshold segmentation based on the image model and adaptive entropy-based method, as well as their combined segmentation, are shown in Figure 2.

The white area in Figure 1 denotes the defect pixels. Images on the first column show that a portion of the defective area cannot be detected by the entropy-based algorithm. This part is detected by the automatic threshold segmentation based on the image model. Images in the fourth

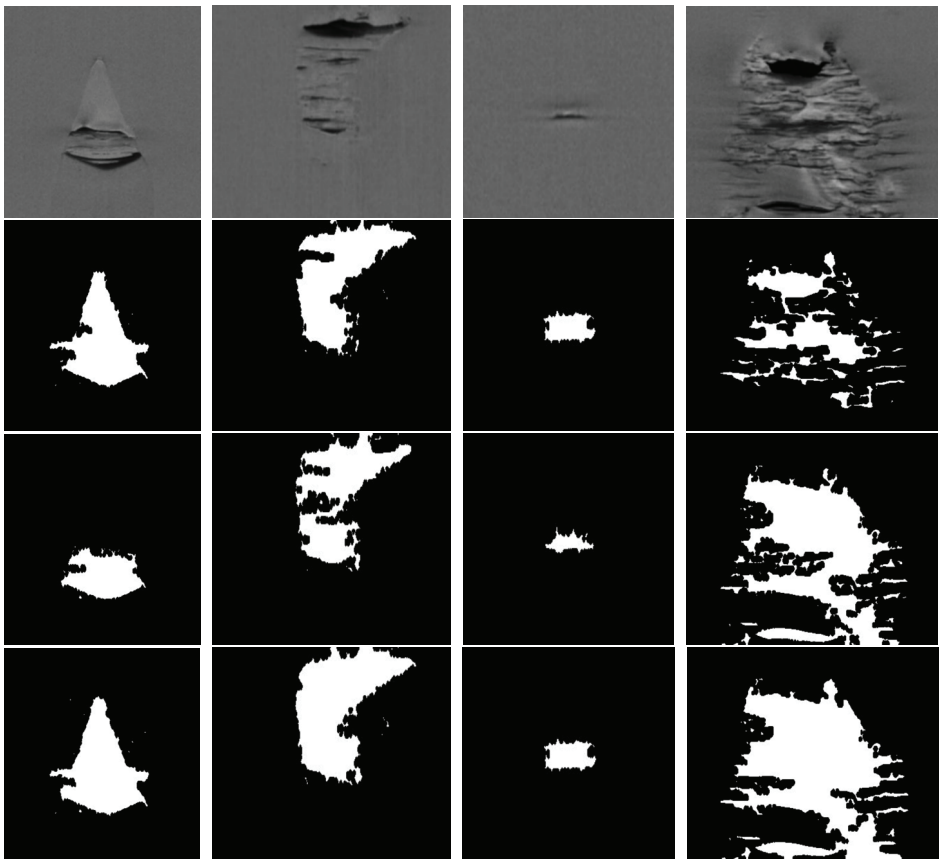

Figure 2. Performance comparison of defect extraction results using different method: 1st row - original images; 2nd row – automatic threshold segmentation based on the image model; 3rd row - adaptive entropy-based segmentation; 4th row - proposed parallel combination segmentation

Table 1. COMPUTATIONAL TIME STATISTICS OF DIFFERENT ALGORITHMS.

Segmentation Algorithm	Minimum time (ms)	Maximum time (ms)	Average time (ms)
Automatic threshold segmentation based on image model	1.10	3.03	2.56
Adaptive entropy-based segmentation	2.33	4.22	3.60
The proposed parallel combination of segmentation	2.53	4.27	3.92

column show that the defect pixels undetected by automatic threshold segmentation are detected by the entropy-based algorithm. The images in the second and third columns indicate the differences in detail of the two single segmentation algorithms. The fusion results of the two segmentation processes in the fourth row show that the difference between the two segmentation processes is unified, the defect region segmented is more complete, and segmentation accuracy is higher.

Considering the real-time detection system in programming, each segmentation algorithm in the program runs in parallel, so the segmentation processing time depends on the maximum value of a single segmentation processing time. The computational time statistics of the proposed method and each single segmentation algorithm have been computed on a PC with an Intel E4500 CPU (2.2 GHz) for the images with sizes between 138 × 256 and 512 × 512, and the results are shown in Table 1. The adaptive entropy-based algorithm requires more time to complete segmentation compared with the automatic thresholding algorithm. However, Prewitt boundary detection allows for fast on-chip implementation and 1D entropy is adopted in this work for efficiency, so the entire image processing time fully meets the real-time requirements[12].

3. Conclusions

This paper presents a parallel combination segmentation method that contains multiple parallel segmentation algorithms. Two sub-segmentation algorithms are designed for high-speed strip surface defect detection, namely, the automatic threshold segmentation algorithm based on the image statistical model and 1D adaptive entropy-based segmentation algorithm. These two algorithms are combined, run in parallel, and their segmentation results are fused to obtain the final segmentation result. The automatic threshold segmentation algorithm and adaptive entropy-based segmentation for most alumina surface defect images can obtain ideal segmentation results. When the results of each algorithm are non-ideal for a few images, their fusion segmentation results can obtain ideal segmentation results. The fusion results are better than the single segmentation results, and the effectiveness of subsequent features calculated and classification accuracy are improved. Many experiments and field applications show that the parallel combination segmentation method is an efficient and stable defect segmentation method superior to each sub-segmentation algorithm.

Acknowledgements

This paper is supported by the Machine Learning Centre of the Suzhou Non-ferrous Metals Research Institute and the School of Aeronautics and Astronautics, Shanghai Jiaotong University.

References

[1] X Jiang, D Mojon, “Adaptive local thresholding by verification-based multithreshold probing with application to vessel detection in retinal images”, IEEE Transactions on Pattern Analysis and Machine Intelligence, IEEE Computer Society, Vol. 25, No. 1, pp. 131–137 , 2003.

[2] Bo Tang, Jianyi Kong, Xingdong Wang, Li Chen, “Surface inspection system of steel strip based on machine vision”, 2009 First International Workshop on Digital Object Identifier, pp. 359-362, 2009.

[3] Weihong Cui, Zequn Guan, Zhiyi Zhang, “An improved region growing algorithm for image segmentation”, 2008 International Conference on Computer Science nd Software Engineering, pp.93-96, December, 2008.

[4] A. Tyagi , M.A. Bayoumi, “Image segmentation on a 2D array by a directed split and merge procedure”, IEEE Transactions on Signal Processing, Vol.40 , Issue. 11, pp. 2804 – 2813

[5] Jingwen Li, Ziping, Zhang, Weili Guo, Hao Su, Wenbing Luo, “A high resolution image segmentation method of a combination of watershed and multi-scale”, Journal of Guangxi Normal University (Natural Science Edition),Vol. 30, No. 2, pp. 40-44, March,2012.

[6] Shung-Shing Lee, Shi-Jinn Horng, Horng-Ren Tsai, “Entropy thresholding and its parallel algorithm on the reconfigurable array of processors with wider bus networks”, IEEE Transactions on image prcessing, Vol.8, NO. 9, pp. 1229-1241, September 1999.

[7] C.I Chang, Y. Du, J. Wang, S.-M. Guo P.D. Thouin, “Survey and comparative analysis of entropy and relative entropy thresholding techniques,” IEE Proceedings of Vision, Image and Signal, Vol. 153, No. 6, pp. 837-850, December 2006.

[8] Cover, T., J. Thomas, Elements of information theory，JohnWiley & Sons, Inc., 1991

[9] J. N. Kapur, P. K. Sahoo, A. K. C. Wong, “New method for gray-level picture thresholding using the entropy of the Hisogram,” Comp Vision, Graphics and Image Proc., Vol.29, pp.273-285, 1985.

[10] R. Gonzalez, R. Woods, Digital Image Processing, Addison-Wesley Publishing Company, 1992.

[11] Rein van den Boomgaard, Richard van Balen, “Methods for fast morphological image transforms using bitmapped images”, Computer Vision, Graphics, and Image Processing: Graphical Models and Image Processing, Vol. 54, No. 3, pp. 252-258, May 1992.

[12] Xiuqin Huang, Xinbin Luo, “A real-time algorithm for aluminum surface defect extraction on non-uniform image from CCD camera”, Proceedings of the 2014 International Conference on Machine Learning and Cybernetics, Vol.2, pp.556-561, July, 2014.